

# Isospin flows

M. Di Toro<sup>1,a</sup>, S.J. Yennello<sup>2</sup>, and B.-A. Li<sup>3</sup>

<sup>1</sup> Laboratori Nazionali del Sud INFN, Phys. Astron. Dept. Catania University, Via S. Sofia 62, I-95123 Catania, Italy

<sup>2</sup> Cyclotron Institute, Texas A&M University, College Station, TX 77843, USA

<sup>3</sup> Department of Chemistry and Physics, P.O. Box 419, Arkansas State University, AR 72467-0419, USA

Received: 18 May 2006 /

Published online: 24 October 2006 – © Società Italiana di Fisica / Springer-Verlag 2006

**Abstract.** In this report, we review the isospin dependence of various forms of the collective flow in heavy-ion reactions from Fermi to relativistic energies. The emphasis will be on suggested possible applications in directly exploring the underlying isovector potential and thus the Equation of State (EoS) of asymmetric nuclear matter, in particular in density regions far away from normal conditions. We also discuss forthcoming challenges and opportunities provided by high-energy radioactive beams.

**PACS.** 25.70.-z Low and intermediate energy heavy-ion reactions – 25.75.Ld Collective flow – 21.30.Fe Forces in hadronic systems and effective interactions – 21.65.+f Nuclear matter

## 1 Introduction

Nuclear collective flow is a motion characterized by space-momentum correlations of dynamical origins. It reveals itself in various forms in nuclear reactions. The study of several components of the collective flow in heavy-ion reactions has been found very useful for extracting information about the Equation of State (EoS) of symmetric nuclear matter [1–5]. The isospin flow refers to the dependence of the collective flow on the isospin asymmetry of the reaction system and/or of the reaction products. This isospin dependence of collective flow has been found useful for studying the isospin asymmetric part of the EoS, namely, the symmetry energy, of neutron-rich matter.

We begin by reviewing briefly our current understanding about the EoS of isospin-asymmetric matter. Several forms of the collective flow will then be introduced. Effects of the symmetry energy/potential on collective flows will be examined in the following sections, with an accurate analysis of the corresponding most sensitive observables. Particular attention will be given to the possibility of studying the symmetry term at high baryon density.

## 2 Equation of state of isospin-asymmetric nuclear matter

Here we shortly review the EoS of isospin-asymmetric matter and the related symmetry energy problem. In

asymmetric matter the energy per nucleon, *i.e.* the equation of state, will be a functional of the total ( $\rho = \rho_n + \rho_p$ ) and isospin ( $\rho_3 = \rho_n - \rho_p$ ) densities. In the usual parabolic form in terms of the asymmetry parameter  $I \equiv \rho_3/\rho = (N - Z)/A$  we can define a symmetry energy  $\frac{E_{sym}}{A}(\rho)$ :

$$\frac{E}{A}(\rho, I) = \frac{E}{A}(\rho) + \frac{E_{sym}}{A}(\rho) I^2. \quad (1)$$

The symmetry term gets a kinetic contribution directly from the basic Pauli correlations and a potential contribution from the properties of the isovector part of the effective nuclear interactions in the medium. Since the kinetic part can be exactly evaluated we can separate the two contributions, reducing the discussion just to a function  $F(u)$  of the reduced density  $u \equiv \rho/\rho_0$  linked to the interaction:

$$\begin{aligned} \epsilon_{sym} &\equiv \frac{E_{sym}}{A}(\rho) \equiv \epsilon_{sym}(kin) + \epsilon_{sym}(pot) \\ &= \frac{\epsilon_F(\rho)}{3} + \frac{C}{2} F(u), \end{aligned} \quad (2)$$

with  $F(1) = 1$ , where  $\rho_0$  is the saturation density and the parameter  $C$  is of the order  $C \simeq 32$  MeV to reproduce the  $a_4$  term of the Bethe-Weizsäcker mass formula. The major uncertainties about the EoS and the symmetry energy are due to both our poor knowledge about the isospin dependence of nuclear effective interactions and the limitations of existing many-body techniques. Shown in fig. 1 are the density-dependent symmetry energies predicted by some of the most widely used microscopic many-body theories. It is seen that, at both sub-saturation and

<sup>a</sup> e-mail: ditoro@lns.infn.it

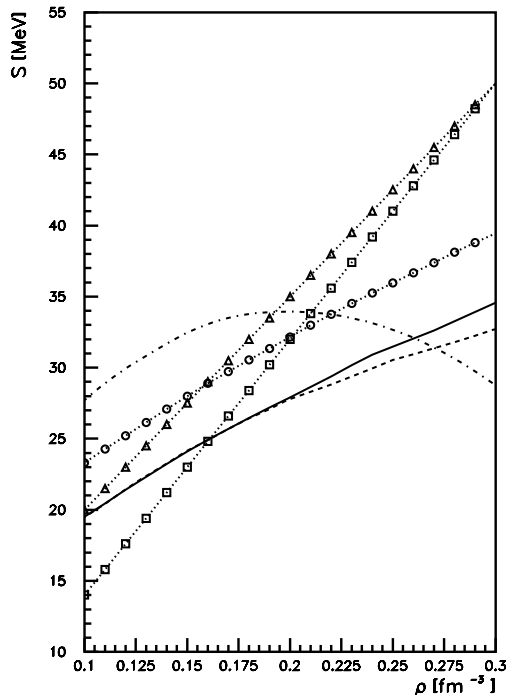


**Fig. 1.** Overview of several theoretical predictions for the symmetry energy  $S$ : Brueckner-Hartree-Fock with Reid93 potential (circles), self-consistent Green function theory with Reid93 potential (full line), variational calculation with Argonne Av14 potential (dashed line), Dirac-Brueckner-Hartree-Fock calculation (triangles), relativistic mean-field model (squares), effective field theory (dash-dotted line). Taken from [6].

supra-saturation densities, the predictions diverge very widely. We note that within each approach the prediction also depends on the two-body effective interaction used and whether/what three-body forces are included. To illustrate the dependence on the effective interactions used, we show in fig. 2 some typical EoSs obtained from Hartree-Fock calculations. It is necessary to stress that they all have the same saturation properties for symmetric NM (top): SKM\* [7,8], SLy230b (SLy4) [9–11] and BPAL32 [12–15]. However, their predictions on the EoS of asymmetric matter, especially their contributions to the potential part of the symmetry energy, are very different. The major challenge is thus to constrain experimentally the potential part of the symmetry energy and the associated symmetry potential. The ultimate goal is to pin down the isospin dependence of nuclear effective interactions that is also responsible for the structure of rare isotopes.

In fig. 2 (bottom) the density dependence of the potential symmetry contribution for the three different effective interactions is reported. While all curves obviously cross at normal density  $\rho_0$ , quite large differences are present for values, slopes and curvatures in low-density and particularly in high-density regions. Moreover, even at the relatively well-known “crossing point” at normal density the

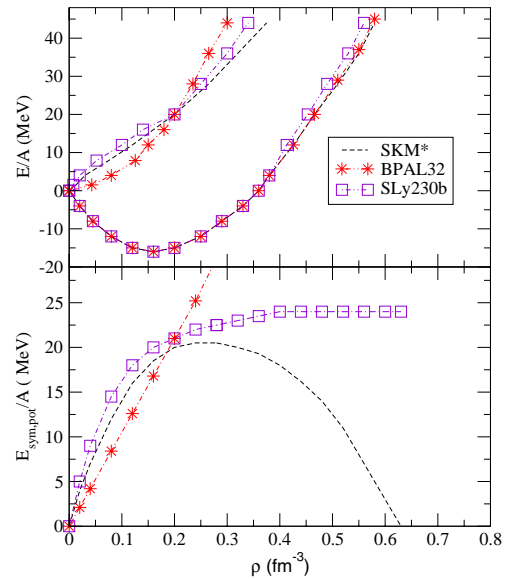


**Fig. 2.** EoS for various effective forces. Top: neutron matter (up), symmetric matter (down); Bottom: potential symmetry term. Taken from [23].

various effective forces are presenting controversial predictions for the momentum dependence of the fields acting on the nucleons and consequently for the splitting of the neutron/proton effective masses, of large interest for nuclear structure and dynamics. In recent years under the stimulating perspectives offered from nuclear astrophysics and from the new Radioactive Ion Beam (RIB) facilities a relevant activity has started in the field of the isospin degree of freedom in heavy-ion reactions, see for review refs. [20–23].

A traditional expansion to second order around normal density is used [18,24,25]

$$\epsilon_{sym} \equiv \frac{E_{sym}}{A}(\rho) = a_4 + \frac{L}{3} \left( \frac{\rho - \rho_0}{\rho_0} \right) + \frac{K_{sym}}{18} \left( \frac{\rho - \rho_0}{\rho_0} \right)^2, \quad (3)$$

in terms of a slope parameter

$$L \equiv 3\rho_0 \left( \frac{d\epsilon_{sym}}{d\rho} \right)_{\rho=\rho_0} = \frac{3}{\rho_0} P_{sym}(\rho_0), \quad (4)$$

which is simply related to the symmetry pressure  $P_{sym} = \rho^2 d\epsilon_{sym}/d\rho$  at  $\rho_0$ , and a curvature parameter

$$K_{sym} \equiv 9\rho_0^2 \left( \frac{d^2\epsilon_{sym}}{d^2\rho} \right)_{\rho=\rho_0}, \quad (5)$$

a kind of symmetry compressibility. We remark that our present knowledge of these basic properties of the symmetry term around saturation is still very poor, see the analysis in ref. [26] and references therein. In particular, we note the uncertainty on the symmetry pressure at  $\rho_0$ , of large importance for structure calculations.

We have seen that asymmetry brings an extra pressure  $P_{sym}$ . For the collective flow discussion it is instructive to

**Table 1.** Symmetry term at saturation.

| $F(u)$      | $L$      | $K_{sym}$ | $[K_{sym} - 6L]$ | $[K_{sym} + 6L]$ |
|-------------|----------|-----------|------------------|------------------|
| const = 1   | +25 MeV  | -25 MeV   | -175 MeV         | +125 MeV         |
| $\sqrt{u}$  | +49 MeV  | -61 MeV   | -355 MeV         | +234 MeV         |
| $u$         | +75 MeV  | -25 MeV   | -475 MeV         | +425 MeV         |
| $u^2/(1+u)$ | +100 MeV | +50 MeV   | -550 MeV         | +650 MeV         |

evaluate the density gradient of the *symmetry pressure* as a function of the slope and curvature of the symmetry term:

$$\frac{d}{d\rho}P_{sym} = \frac{1}{9}(K_{sym} + 6L), \quad (6)$$

that around normal density gives

$$\frac{d}{d\rho}P_{sym} = \left( \frac{10}{27}\epsilon_F + C \left[ \frac{d}{du} + \frac{1}{2} \frac{d^2}{du^2} \right] F(u) \Big|_{u=1} \right). \quad (7)$$

The compressibility of the matter is also modified by the asymmetry [23,27]. For the compressibility shift *at equilibrium* we have, after some algebra,

$$\begin{aligned} \Delta K_{NM}(I) &= 9\rho_0 \left[ \rho_0 \frac{d^2}{d\rho^2} - 2 \frac{d}{d\rho} \right] \epsilon_{sym}(\rho) \Big|_{\rho=\rho_0} I^2 \\ &= [K_{sym} - 6L] I^2 < 0. \end{aligned} \quad (8)$$

We note the different interplay between slope and curvature of the symmetry term for flows, eqs. (6), (7), and monopole, eq. (8), observables. In order to have a quantitative idea, we now show explicitly the influence on the  $L, K_{sym}$  parameters of a different density dependence in the potential part of the symmetry energy around saturation, *i.e.* of the function  $F(u)$  of eq. (2):

$$\begin{aligned} L &= \frac{2}{3}\epsilon_F + \frac{3}{2}C \frac{d}{du} F(u) \Big|_{u=1}, \\ K_{sym} &= -\frac{2}{3}\epsilon_F + \frac{9}{2}C \frac{d^2}{du^2} F(u) \Big|_{u=1}. \end{aligned}$$

We obtain the rather instructive table 1 for various functional forms  $F(u), u \equiv \rho/\rho_0$ , around  $\rho_0$ . A stiffer symmetry term in general enhances the pressure gradient of asymmetric matter. We can expect direct effects on the nucleon emissions in the reaction dynamics, fast particles and collective flows. In particular, we will see larger flows in isospin-asymmetric collisions. Moreover, due to the different fields seen by neutrons and protons, we shall observe even specific isotopic effects.

In fig. 3 we report, for an asymmetry  $(N-Z)/A = 0.2$  representative of  $^{124}\text{Sn}$ , the density dependence of the symmetry contribution to the mean-field potential for the different effective interactions in the isovector channel. It is seen that in regions just off normal density the field “seen” by neutrons and protons in the three cases is very different. We thus expect important isospin effects on nucleon transport during reactions at intermediate energies (prompt particle emissions, collective flows,  $n/p$  interferometry) where the interacting asymmetric nuclear matter

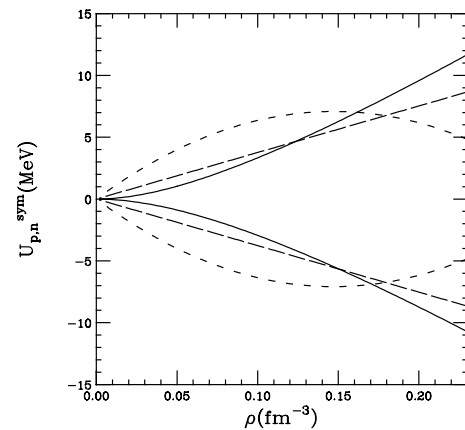


**Fig. 3.** Symmetry contribution to the mean field at  $I = 0.2$  for neutrons (upper curves) and protons (lower curves): dashed lines “asy-soft”, long-dashed lines “asy-stiff”, solid lines “asy-superstiff”. Taken from [23].

will experience compressed and expanding phases. These points have been analysed in some detail using isospin-dependent transport simulations for the reaction dynamics. We always compare results obtained with forces that have *the same saturation properties for symmetric NM*. We will refer to an “*asy-stiff*” EoS (*e.g.*, like BPAL32 of fig. 2). when we are considering a potential symmetry term linearly increasing with nuclear density and to a “*asy-soft*” EoS (*e.g.*, like SKM\* of fig. 2) when the symmetry term shows a saturation and eventually a decrease above normal density. In some cases, in order to enhance the dynamical effects, we will consider also “*asy-superstiff*” behaviours, *i.e.* with a roughly parabolic increase of the symmetry term above normal density [15,28,29].

### 3 Collective flows: definitions

The collective motion can be characterized in several ways that pin down different space-momentum correlations that can be generated by the dynamics. The kind of collective flows that have been suggested and employed to get information on the equation of state can be divided into three categories: radial, sideward and elliptic. The sideward and elliptic flows have been and are currently useful tools for the study of the compressibility of symmetric nuclear matter. In the search for the density behaviour of the symmetry energy, similar concepts can be exploited but high-lightening the difference between neutrons and protons or light clusters with different isospin. We will define

the different types of collective flow and we will discuss the current status of the effects expected due to different  $E_{sym}(\rho)$ , and related momentum dependence. We will see that first experimental results with stable beam already show hints of the effect of the symmetry energy. Thus future, more exclusive, experiments with radioactive beams should be able to set stringent constraints on the density dependence of the symmetry energy far from ground-state nuclear matter.

The sideward (transverse) flow is a deflection of forward- and backward-moving particles, within the reaction plane [30]. It is formed because for the compressed and excited matter it is easier to get out on one side of the beam axis than on the other. The sideward flow is often represented in terms of the average in-plane component of the transverse momentum at a given rapidity  $\langle p_x(y) \rangle$ :

$$F(y) \equiv \frac{1}{N(y)} \sum_{i=1}^{N(y)} p_{x_i} \equiv \langle p_x(y) \rangle. \quad (9)$$

The particular case in which the slope of the transverse flow is vanishing in a region around midrapidity is referred to as balance energy. It comes out from a balance between the attraction of the mean field and the repulsion of the two-body collisions.

The build up of sideward and elliptic flow is realized around the higher-density stage of the reaction and thus is a powerful tool for the search of the high-density behaviour of the symmetry energy. It represents a very general means of investigation, giving information on the dynamical response of excited nuclear matter in heavy-ion collisions, from the Fermi energies [1–5] up to the ultrarelativistic regime, in the search for a phase transition to QGP [31]. For the isospin effect the sum over the particles in eq. (9) is separated into protons and neutrons. In refs. [29,32] also the neutron-proton differential flow  $F^{pn}(y)$  has been suggested as a very useful probe of the isovector part of the EoS since it appears rather insensitive to the isoscalar potential and to the in-medium nuclear cross-section and, as we will discuss, it combines the isospin distillation effects with the direct dynamical flow effect. The definition of the differential flow  $F_{pn}(y)$  is

$$F_{pn}(y) \equiv \frac{1}{N(y)} \sum_{i=1}^{N(y)} p_{x_i} \tau_i \equiv \frac{N_n}{N(y)} F_n(y) - \frac{N_p}{N(y)} F_p(y), \quad (10)$$

where  $N(y)$  is the total number of free nucleons at rapidity  $y$  ( $N_{n,p}$ , neutron/proton multiplicities) and  $p_{x_i}$  is the transverse momentum of particle  $i$  in the reaction plane ( $\tau_i$  is +1 and -1 for protons and neutrons). The flow observables can be seen, respectively, as the first and second coefficients from the Fourier expansion of the azimuthal distribution [33]:

$$\frac{dN}{d\phi}(y, p_t) \propto 1 + 2V_1 \cos(\phi) + 2V_2 \cos(2\phi),$$

where  $p_t = \sqrt{p_x^2 + p_y^2}$  is the transverse momentum and  $y$  the rapidity along beam direction. The transverse flow

can be also expressed as

$$V_1(y, p_t) = \left\langle \frac{p_x}{p_t} \right\rangle.$$

It provides information on the azimuthal anisotropy of the transverse nucleon emission and has been used to study the EoS and cross-section sensitivity of the balance energy [32].

The second coefficient of the expansion defines the elliptic flow  $v_2$  that can be expressed as

$$V_2(y, p_t) = \left\langle \frac{p_x^2 - p_y^2}{p_t^2} \right\rangle.$$

It measures the competition between in-plane and out-of-plane emissions. The sign of  $V_2$  indicates the azimuthal emission anisotropy: particles can be preferentially emitted either in the reaction plane ( $V_2 > 0$ ) or out-of-plane (*squeeze-out*,  $V_2 < 0$ ) [33,34]. The  $p_t$ -dependence of  $V_2$ , which has been recently investigated by various groups [5, 34–36], is very sensitive to the high-density behavior of the EoS since highly energetic particles ( $p_t \geq 0.5$ ) originate from the initial compressed and out-of-equilibrium phase of the collision, see, *e.g.*, ref. [36]. Also at high energy it is allowing to get insight of the partonic stage and hadronization mechanism in ultrarelativistic heavy-ion collisions [31].

#### 4 Collective flows at the Fermi energies: isospin effects around the balance energy

The Fermi energy range (roughly from 20 to 100 A MeV beam energies), transitional region from a mean field to a  $NN$ -collision dynamics with the related building up of density gradients, represents a kind of threshold for out-of-plane flows (radial and elliptic). Meanwhile the transverse flow shows the *balance* effect, *i.e.* it changes from negative to positive due to the competition between the attractive mean field and the repulsive  $NN$  collisions (plus Coulomb), see [3]:

$$\frac{dF(y)}{dy}(E_{bal})_{y=0} = 0.$$

Due to this delicate balance one would expect isospin effects on the mean field to be relevant.

The isospin dependence of the transverse collective flow near the balance energy was first pointed out in ref. [37], where it is stressed that the reactions involving neutron-rich nuclei should have a significantly stronger attractive flow and consequently a higher balance energy. Shown in fig. 4 is the impact parameter dependence of the flow parameter for the reaction of  $^{58}\text{Fe} + ^{58}\text{Fe}$  and  $^{58}\text{Ni} + ^{58}\text{Ni}$  at a beam energy of 55 MeV/nucleon from experiments done at MSU [38–40]. It is interesting to see that the flow parameter for the neutron-richer system is consistently higher and is in agreement with transport model predictions [37]. Pak *et al.* have also studied the

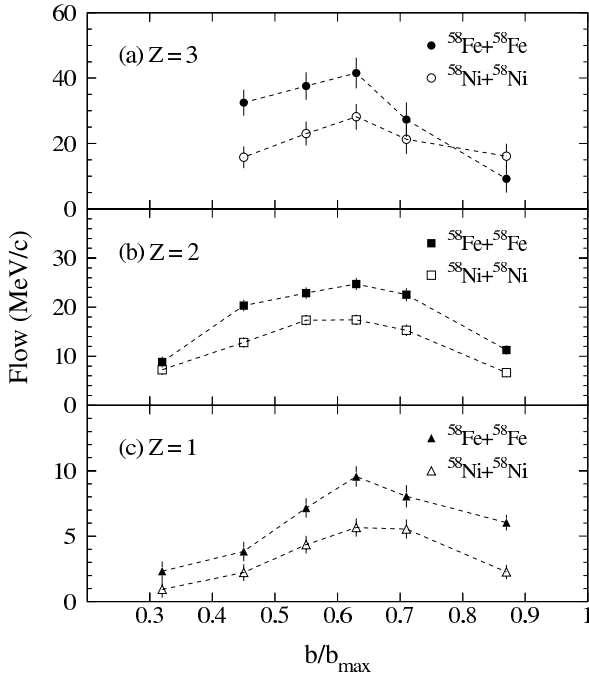


**Fig. 4.** Flow parameters for the reactions of  $^{58}\text{Fe} + ^{58}\text{Fe}$  and  $^{58}\text{Ni} + ^{58}\text{Ni}$  as a function of the reduced impact parameter at a beam energy of 55 MeV/nucleon. Taken from ref. [39].

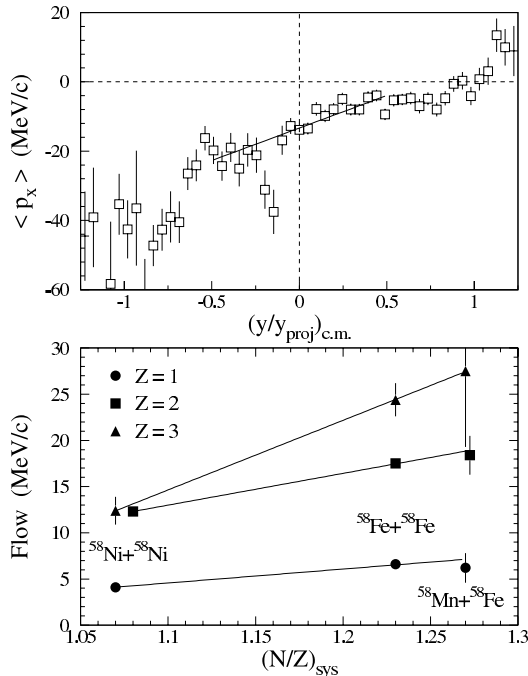


**Fig. 5.** Upper window: mean transverse momentum in the reaction plane *versus* the reduced c.m. rapidity for  $Z = 2$  fragments from impact-parameter-inclusive  $^{58}\text{Mn} + ^{58}\text{Fe}$  collisions at 55 MeV/nucleon. Lower window: isospin dependence of the flow parameter for inclusive collisions at a beam energy of 55 MeV/nucleon. Taken from ref. [39].

flow parameter as a function of the isotope ratio of the composite projectile plus target system for three different fragment types from three isotopic entrance channels. Shown in the upper window of fig. 5 is the mean transverse momentum in the reaction plane *versus* the reduced c.m. rapidity for  $Z = 2$  fragments from impact-parameter-inclusive  $^{58}\text{Mn} + ^{58}\text{Fe}$  collisions at 55 MeV/nucleon. The flow parameter extracted for inclusive events is plotted in the lower window of fig. 5 as a function of the ratio of neutrons to protons of the combined system  $(N/Z)_{\text{cs}}$ . The flow parameter increases linearly with the ratio  $(N/Z)_{\text{cs}}$  for all three types of particles.

In spite of the low  $^{58}\text{F}$  asymmetry ( $I = 0.1$ ), in the isospin-transport simulations of ref. [41] the shift of the balance energy is getting a noticeable contribution from the stiffness of the symmetry term. This is shown in fig. 6, where the flow slope at midrapidity *vs.* beam energy is reported: an *asy-stiff* behavior, more attractive for protons above normal density for the Fe asymmetric case, gives a clear shift in the balance energy as well as a larger (negative) flow at 55 AMeV, *i.e.* below the balance. Both effects are in agreement with the data and are disappearing in the *asy-soft* choice. Of course also the isospin and density dependence of the  $NN$  cross-sections is important (see the (c), (d) plots) but we note that a good sensitivity to the isovector part of the EoS is still present. In particular, we can see that the isospin dependence of the mean field is able to keep the transverse flow difference between protons in Fe-Fe and Ni-Ni. However a systematic study over different systems with more “exotic” isospin content is necessary to confirm this result. An important effect predicted by the simulations is the clear difference between

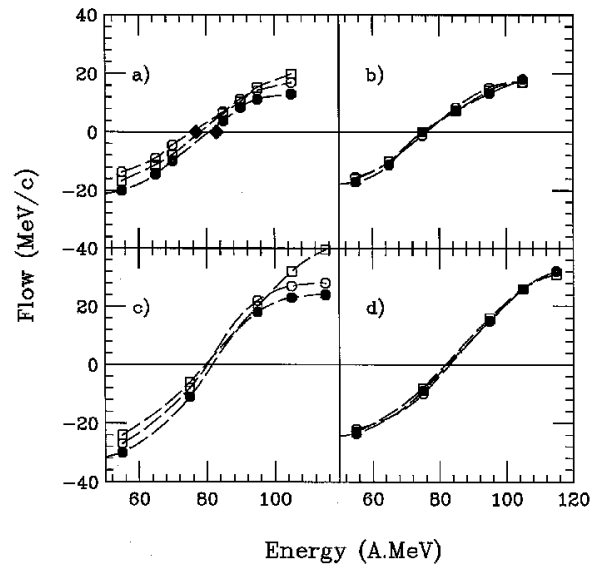


**Fig. 6.** Energy dependence of flows at  $b_{\text{red}} = 0.45$  [42]: Fe + Fe protons (full circles); Ni + Ni protons (open circles); Fe + Fe neutrons (squares). (a) Asy-stiff; (b) asy-soft; (c), (d) same for  $\sigma_{NN} = 2 \text{ fm}^2$  no isospin dependent. The full diamonds in (a) represent the proton balance energy data of ref. [38] for the Fe + Fe (right) and Ni + Ni systems. Taken from [41].

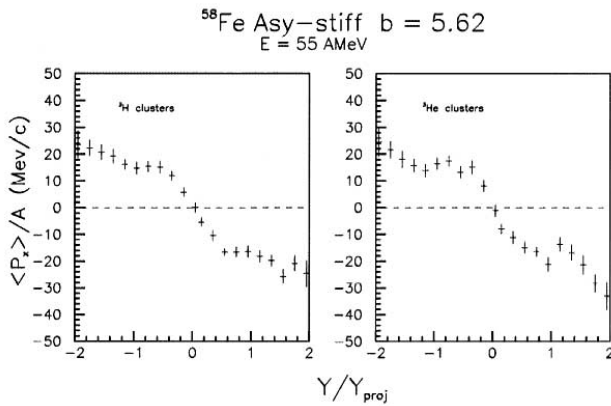


**Fig. 7.** Mean transverse momentum in the reaction plane *vs.* reduced rapidity for light  ${}^3\text{He}$ - ${}^3\text{H}$  isobars in the Fe + Fe collisions at 55 A MeV beam energy (*i.e.* below the balance) for semicentral impact parameter,  $b_{red} = 0.6$ . Asy-stiff parametrization. Taken from [41].

neutron and proton flows. Due to the difficulties in measuring neutrons this should be seen in a detailed study of light isobar flows. Moreover, we like to recall that clusters are better probing the higher-density regions. This point is quantitatively shown in fig. 7 where we present the transverse momentum *vs.* rapidity distributions for  ${}^3\text{He}$ -triton clusters in semicentral Fe-Fe collisions at 55 A MeV, *i.e.* below the balance energy [41]. We can estimate a 20% larger (negative) flow for the  ${}^3\text{He}$  ions, just opposite to what is expected from Coulomb effects. This appears to be a clear indication of the contribution of a much reduced (negative) neutron flow in the case of an *asy-stiff* force, *i.e.* a more repulsive symmetry term just above  $\rho_0$ . The effect would disappear in an *asy-soft* choice.

For heavier systems, with much larger Coulomb repulsion, the flow balance is at lower energies. The Iso-EoS effects are less evident for two main reasons: i) the smaller relative weight of symmetry *vs.* Coulomb contributions; ii) the reduced compression in the interacting region. This is clearly shown in fig. 8, from the iso-transport simulations of ref. [43], where the proton transverse flows for the  ${}^{124}\text{Sn} + {}^{124}\text{Sn}$  case at 50 A MeV (semicentral) are reported. There is no appreciable difference in the evaluations with two quite different density dependencies of the symmetry term,  $F(u) = u^\gamma$ ,  $u \equiv \rho/\rho_0$ ,  $\gamma = 0.5$  (rather *asy-soft*) and  $\gamma = 2$  (*asy-superstiff*).

Moreover, at the Fermi energies free nucleons can be emitted from various sources, from the early high-density stage as well as in the expansion phase, when fragments are formed (isofractionation or isodistillation) and finally from excited primary clusters. For the Iso-EoS studies more exclusive flow data are needed. In particular, a good selection for the source density could be based on the transverse momentum of the nucleons emitted at a given rapidity. The proton elliptic flow appears very sensitive to this analysis, see fig. 8 for the same Sn + Sn *n*-rich system [43]. At high  $p_t$ 's the Iso-EoS differences are evident, with a reduced squeeze-out flow in the  $\gamma = 2$  case. At this

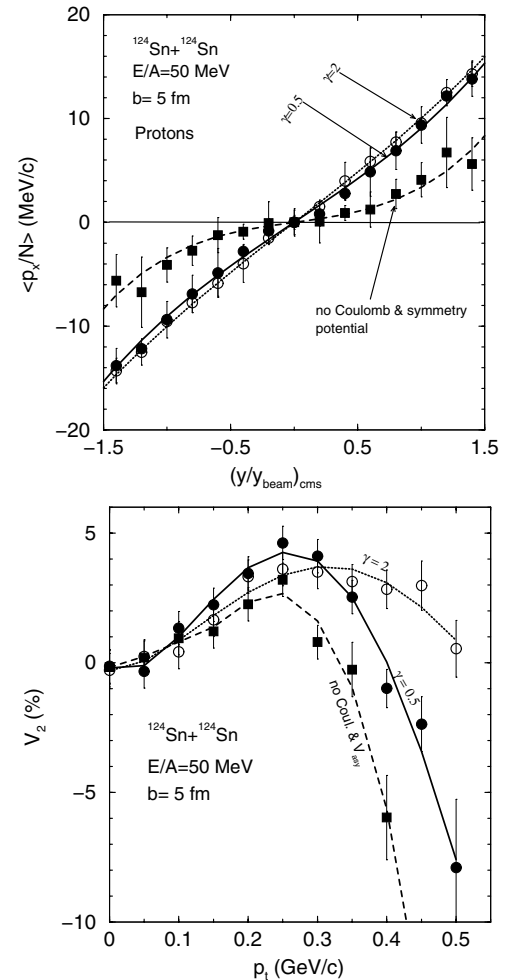


**Fig. 8.** Top: mean transverse momentum in the reaction plane *vs.* reduced rapidity for protons in the  ${}^{124}\text{Sn} + {}^{124}\text{Sn}$  collisions at 50 A MeV beam energy (*i.e.* just above the balance) for semicentral impact parameter,  $b_{red} = 0.6$ . Bottom: elliptic flow for midrapidity protons as a function of transverse momentum. Two different symmetry energy parametrizations are used (see text). From ref. [43].

low energy the less repulsive interactions (no Coulomb and symmetry potentials) give the largest squeeze-out, just opposite to what we will see at higher energies. Finally, we note that high-momentum particles will better probe the momentum dependence of the mean field, including its isospin-dependent part. This is the subject of the next section.

Despite the possible interpretation, in order to make the analysis of collective flow more sensitive to the symmetry potential, the *neutron-proton* differential flow, defined in eq. (10), has been introduced [32]. In such a way one combines constructively the difference in the neutron-proton collective flow and the difference in the number of protons and neutrons emitted. At the same time the influences of the isoscalar potential and the in-medium nucleon-nucleon cross-sections are also reduced. However, the measurement of such a differential flow demands not

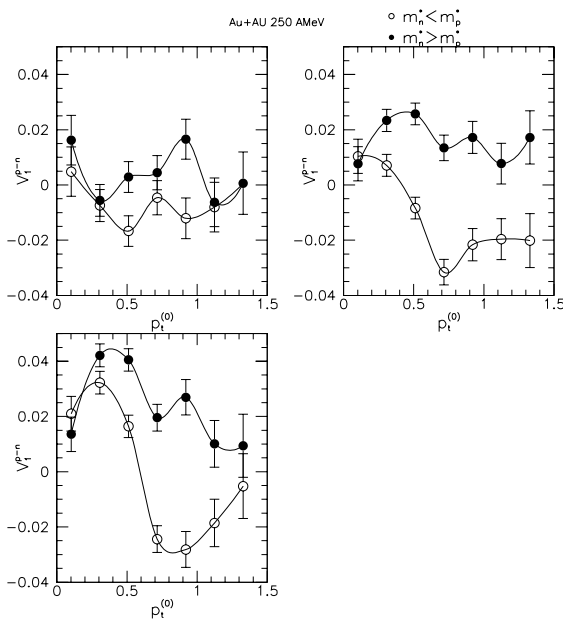


**Fig. 9.** Difference between proton and neutron  $V_1$  flows in a semicentral reaction Au + Au at 250 AMeV for three rapidity ranges. Upper left panel:  $|y^{(0)}| \leq 0.3$ ; upper right:  $0.3 \leq |y^{(0)}| \leq 0.7$ ; lower left:  $0.6 \leq |y^{(0)}| \leq 0.9$ . Taken from [47].

only for, the measurement of neutron collective flow but also for a precise assessment of their number, which most likely is impossible. On the other hand, the idea to combine more than one isospin contribution in one observable is certainly important for elusive effects as those coming from the symmetry energy. In this respect, we would like to note that the usual problems caused by the neutrons can be overcome by looking at clusters. For example, one can use the definition of differential collective flow and apply it to the  ${}^3\text{H}$ - ${}^3\text{He}$  isospin doublet, see previous discussion.

## 5 Effective mass splitting and collective flows

The problem of momentum dependence (MD) in the isospin channel is still very controversial and it would be extremely important to get more definite experimental information, see the recent refs. [44–49]. Intermediate energies are important in order to have high-momentum particles and to test regions of high baryon (isoscalar) and isospin (isovector) density during the reaction dynamics. Now, we present some qualitative features of the dynamics in heavy-ion collisions in higher-energy regions, of large interest for the RIA facility, related to the splitting of nucleon effective masses.

Collective flows are very good candidates since they are expected to be very sensitive to the momentum dependence of the mean field, see [23,34] and references therein. We have then tested the isovector part of the momentum dependence just evaluating the *difference* of

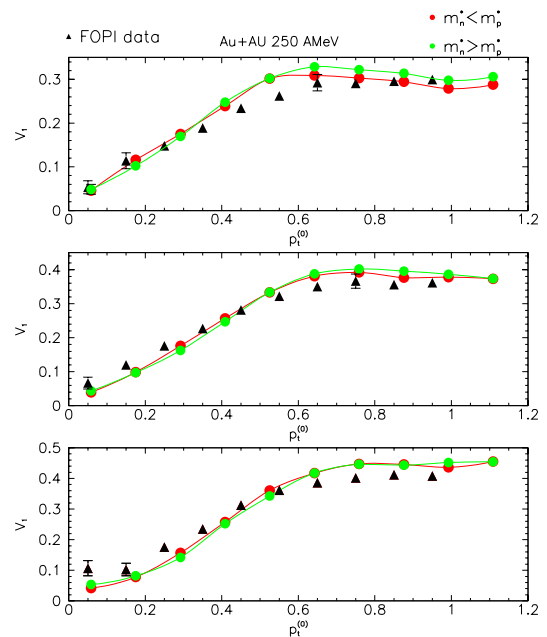


**Fig. 10.** Comparison of the  $V_1$  proton flow with FOPI data [50] for three rapidity ranges. Top:  $0.5 \leq |y^{(0)}| \leq 0.7$ ; center:  $0.7 \leq |y^{(0)}| \leq 0.9$ ; bottom:  $0.9 \leq |y^{(0)}| \leq 1.1$ . Taken from [47].

neutron/proton transverse and elliptic flows

$$V_{1,2}^{(n-p)}(y, p_t) \equiv V_{1,2}^n(y, p_t) - V_{1,2}^p(y, p_t)$$

at various rapidities and transverse momenta in semicentral ( $b/b_{max} = 0.5$ )  ${}^{197}\text{Au} + {}^{197}\text{Au}$  collisions at 250 AMeV, where some proton data are existing from the FOPI Collaboration at GSI [50,51].

We report here on expected effects of the isospin MD, studied by means of the Boltzmann-Nordheim-Vlasov transport code, refs. [52,53], implemented with a *BGBD-like* [54,55] mean field with a different  $(n, p)$  momentum dependence, see refs. [44,47], that allow to follow the dynamical effect of opposite  $n/p$  effective mass splitting while keeping the same density dependence of the symmetry energy.

### Transverse flows

For the difference of nucleon transverse flows, see fig. 9, the mass splitting effect is evident at all rapidities, and nicely increasing at larger rapidities and transverse momenta, with more neutron flow when  $m_n^* < m_p^*$ . Just to show that our simulations give realistic results we compare in fig. 10 with the proton data of the FOPI Collaboration for similar selections of impact parameters rapidities and transverse momenta. The agreement is quite satisfactory. We see a slightly reduced proton flow at high transverse momenta in the  $m_n^* < m_p^*$  choice, but the effect is too small to be seen from the data. Our suggestion of measuring just the difference of  $n/p$  flows looks much more promising. Similar calculations have been performed in ref. [45] for the  ${}^{132}\text{Sn}$ - ${}^{124}\text{Sn}$  system at 400 AMeV beam

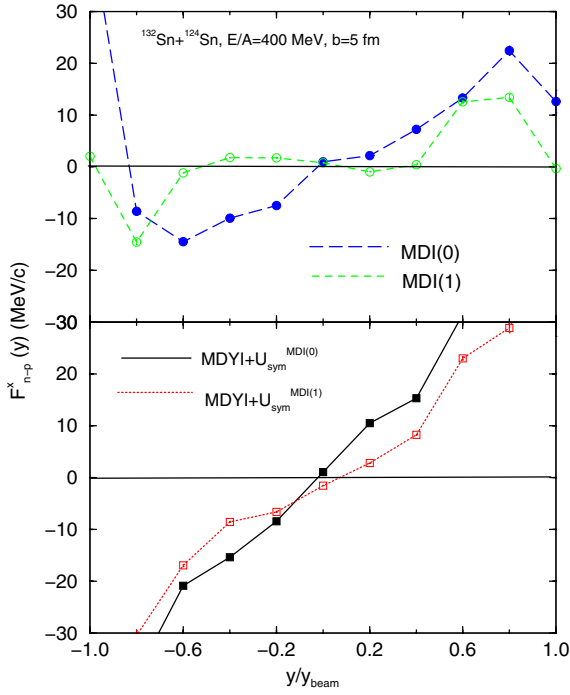


**Fig. 11.** Neutron-proton differential transverse flows *vs.* reduced rapidity with (upper panel) and without (lower panel) the momentum dependence of the symmetry potential for  $^{132}\text{Sn} + ^{124}\text{Sn}$  collisions at 400 A MeV beam energy and semicentral impact parameter  $b = 5$  fm. Two different density parametrizations of the symmetry energy were used as indicated, see also text. Taken from [45].

energy. The *differential* transverse flow, eq. (10), is shown in fig. 11 with and without the *isospin-MD* of the mean field. The effect of the nucleon mass splitting is less evident. This could be related to the choice  $m_n^* > m_p^*$  in this calculation, which tends to reduce symmetry effects on high momentum particles.

### Elliptic flows

The same analysis has been performed for the difference of elliptic flows, see fig. 12. Again the mass splitting effects are more evident for different rapidity and transverse momentum selections. In particular, the differential elliptic flow becomes systematically negative at low rapidities when  $m_n^* < m_p^*$ . This is revealing a faster neutron emission from the high-density region and so a larger neutron squeeze out (more spectator shadowing) for high-energy collisions. In fig. 13 we also show a comparison with recent proton data from the FOPI Collaboration. The agreement is still satisfactory. As expected the proton flow is more negative (more proton squeeze-out) when  $m_n^* > m_p^*$ . It is however difficult to draw definite conclusions only from proton data.

Again the measurement at least of a  $n/p$  flow difference appears essential. This could be in fact an experimental problem due to the difficulties in measuring neutrons. Our suggestion is to measure the difference between light

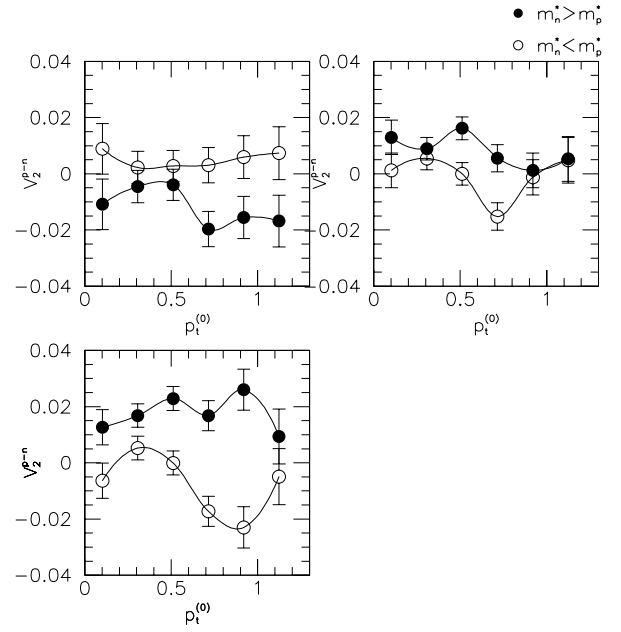


**Fig. 12.** Difference between proton and neutron elliptic flows for the same semicentral reaction Au + Au at 250 A MeV and rapidity ranges as in fig. 9. Taken from [47].

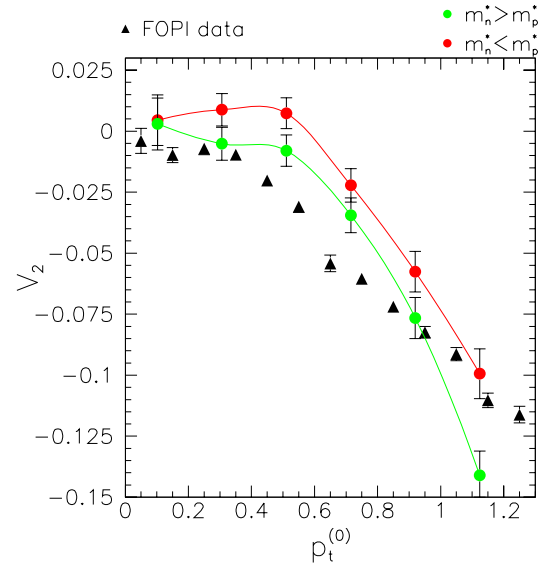


**Fig. 13.** Comparison of the elliptic proton flow with FOPI data [51] (M3 centrality bin,  $|y^{(0)}| \leq 0.1$ ). Taken from [47].

isobar flows, like triton *vs.*  $^3\text{He}$  and so on. We expect to clearly see the effective mass splitting effects, may be even enhanced due to larger overall flows shown by clusters, see [23,41].

## 6 Collective flows as probes of the high-density symmetry energy

Relativistic heavy-ion collisions open the unique possibility to explore the Equation of State (EoS) of nuclear



matter far from saturation, in particular the density dependence of the symmetry energy [23]. The elliptic flows of nucleons and light isobars appear to be quite sensitive to the microscopic structure of the symmetry term, in particular, for particles with large transverse momenta, since they represent an earlier emission from a compressed source. Thus future, more exclusive, experiments with relativistic radioactive beams should be able to set stringent constraints on the density dependence of the symmetry energy far from ground-state nuclear matter. In recent years some efforts have been devoted to the effects of the scalar-isovector channel in finite nuclei. Such investigations have not shown a clear evidence for the  $\delta$ -field and this can be understood considering that in finite nuclei one can test the interaction properties mainly below the normal density, where the effect of the  $\delta$ -channel on symmetry energy and on the effective masses is indeed small [18] and eventually could be absorbed into nonlinear terms of the  $\rho$ -field. Moreover, even studies of the asymmetric nuclear matter by means of the Fermi-liquid theory [18] and a linear response analysis have concluded that some properties, like the borderline and the dynamical response inside the spinodal instability region, are not affected by the  $\delta$ -field [19]. Here we show that heavy-ion collisions around 1 AGeV with radioactive beams can provide instead a unique opportunity to spot the presence of the scalar isovector channel [56]. In fact, due to the large counterstreaming nuclear currents one may exploit the different Lorentz nature of a scalar and a vector field. Oversimplifying the heavy-ion collision dynamics we consider locally neutrons and protons with the same  $\gamma$  factor (*i.e.* with the same speed). Then nucleon equations of motion can be expressed approximately by the following transparent form ( $\rho_{S3} = \frac{M^*}{E^*} \rho_3$ ), [56]:

$$\frac{d\mathbf{p}_p^*}{d\tau} - \frac{d\mathbf{p}_n^*}{d\tau} \simeq 2 \left[ \gamma f_\rho - \frac{f_\delta}{\gamma} \right] \nabla \rho_3, \quad (11)$$

where  $\gamma$  is the Lorentz factor for the collective motion of a given ideal cell. Keeping in mind that  $NL\rho\delta$  has a three times larger  $\rho$ -field [18], it is clear that dynamically the vector-isovector mean field acting during the heavy-ion collision is much greater than the one of the  $NL\rho, NLD\rho$  cases ( $NLD\rho$  is built with the same density dependence of the  $NL\rho\delta$  symmetry energy, but without the  $\delta$  coupling). Then the isospin effect is mostly caused by the different Lorentz structure of the “interaction” which results in a dynamical breaking of the balance between the  $\rho$  vector and  $\delta$  scalar fields, present in nuclear matter at equilibrium. The Catania group has performed a set of relativistic transport simulations for the realistic  $^{132}\text{Sn} + ^{124}\text{Sn}$  reaction at 1.5 AGeV ( $b = 6\text{fm}$ ), that likely could be studied with the new planned radioactive beam facilities at intermediate energies. The transverse and elliptic differential flows are shown in fig. 14. The effect of the different structure of the isovector channel is quite clear. Particularly evident is the splitting in the high- $p_t$  region of the elliptic flow. From fig. 14 we see that, in spite of the statistical errors, in the  $(\rho + \delta)$  dynamics the high- $p_t$  neutrons show a much larger *squeeze-out*. This is fully consistent

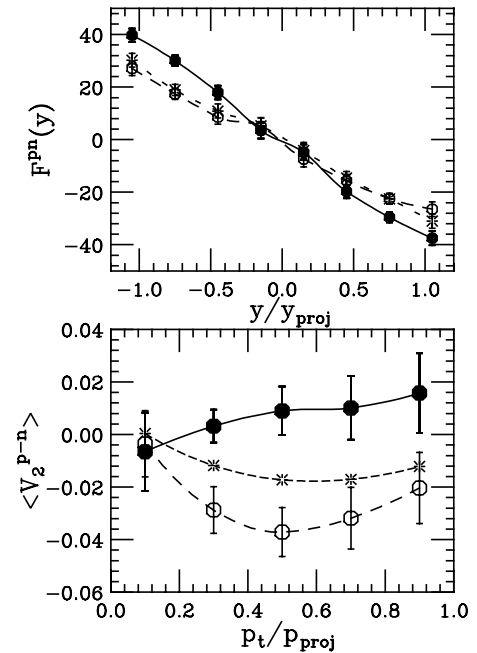


**Fig. 14.** Differential neutron-proton flows for the  $^{132}\text{Sn} + ^{124}\text{Sn}$  reaction at 1.5 AGeV ( $b = 6\text{fm}$ ) from the three different models for the isovector mean fields. Top: transverse flows. Bottom: elliptic flows. Full circles and solid line:  $NL\rho\delta$ . Open circles and dashed line:  $NL\rho$ . Stars and short dashed line:  $NL-D\rho$ . Error bars: see the text. Taken from [56].

with an early emission (more spectator shadowing) due to the larger repulsive  $\rho$ -field. We can expect this appreciable effect since the relativistic enhancement discussed above is relevant just at the first stage of the collision. The  $v_2$  observable, which is a good *chronometer* of the reaction dynamics, appears to be particularly sensitive to the Lorentz structure of the effective interaction. We expect similar effects, even enhanced, from the measurements of differential flows for light isobars, like  $^3\text{H}$  *vs.*  $^3\text{He}$ .

Predictions have also been made with several other transport models. Shown in fig. 15 is the  $n$ - $p$  differential flow for the reaction of  $^{132}\text{Sn} + ^{124}\text{Sn}$  at a beam energy of 400 MeV/nucleon and an impact parameter of 5 fm [57]. Effects of the symmetry energy are clearly revealed by changing the symmetry energy labeled with the parameter  $x$  in fig. 15. It is worth mentioning that the isospin dependence of radial flow at RIA energies has also been investigated very recently [58]. The difference in the radial flow velocity for neutrons and protons is the largest for the stiffest symmetry energy as one expects. As the symmetry energy becomes softer the difference disappears gradually. However, the overall effect of the symmetry energy on the radial flow is small, even for the stiffest symmetry energy with  $x = -2$  the effect is only about 4%. This is because the pressure of the participant region is dominated by the kinetic contribution. Moreover, the compressional contribution to the pressure is overwhelmingly dominated by the isoscalar interactions. For protons, the radial flow

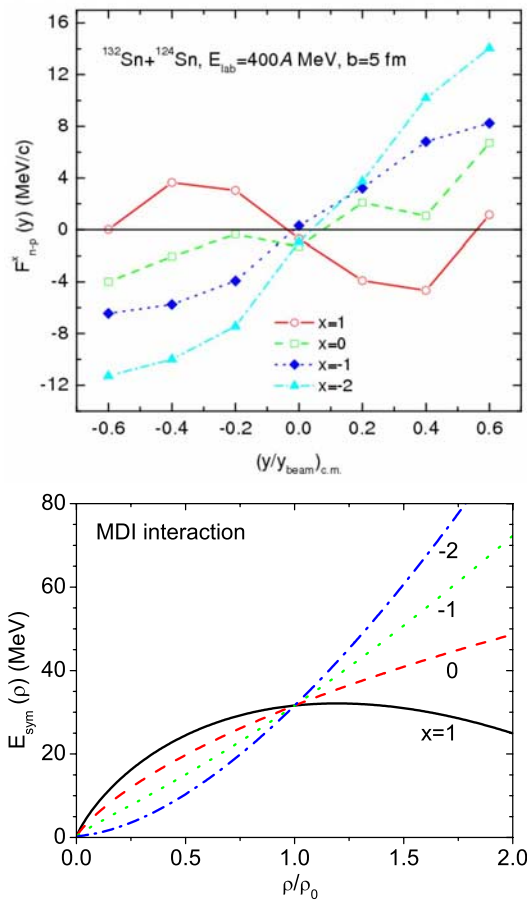


**Fig. 15.** Neutron-proton differential flow at RIA and GSI energies (top panel) and symmetry energy used in obtaining the above results (bottom panel). Taken from [57].

is affected much more by the Coulomb potential than the symmetry potential. In fact, the Coulomb potential almost cancels out the effect of the symmetry potential at  $x = -2$ . As the symmetry energy becomes softer, the radial flow for protons becomes higher than that for neutrons. The radial flow thus seems to be less useful for studying the EoS of neutron-rich matter.

## 7 Conclusions

The EoS of neutron-rich matter has been a long-standing fundamentally important topic in both nuclear physics and astrophysics. Nuclear reactions induced by neutron-rich nuclei provide a great opportunity to pin down the EoS of neutron-rich matter. In particular, the isospin dependence of various components/forms of nuclear collective flow is very useful for extracting interesting information about the EoS of neutron-rich matter. Some experimental evidence indicating the isospin dependence of collective flow has been obtained from heavy-ion reactions at the Fermi energies. In particular, it was shown both theoretically and experimentally that the flow strength of charged particles depends on the isospin asymmetry of the

reaction system. Moreover, the balance energy where the collective flow vanishes is also isospin dependent. A number of interesting predictions regarding the isospin flows have been made using isospin-dependent transport models. However, there are currently very few experimental data available to be compared with. Because of the fact that the isovector potential is rather small compared to the isoscalar potential during heavy-ion reactions, many of the sensitive observables use differences between neutrons and protons, such as the neutron-proton differential transverse and/or elliptic flow. They thus require the detection of neutrons simultaneously with charged particles. Although it is challenging to measure low-energy neutrons accurately, the transverse flow and squeeze-out of neutrons have been measured at both GSI and the Bevalac. In fact, neutron detectors have been built/planned at several radioactive beam facilities. One can thus expect to see high-quality neutron-proton differential flow data coming in the next few years. In the meantime, observables using differences of light isobaric nuclei can also provide some useful information albeit less sensitive than neutrons and protons.

While we have concentrated on the collective flow observables in this report, the readers are kindly reminded that there are many other equally useful observables, such as, the  $n/p$  ratio of pre-equilibrium nucleon emissions,  $\pi^-/\pi^+$  and  $K^0/K^+$  ratios as well as neutron-proton correlation functions, for studying the EoS of isospin-asymmetric matter. Correlations of multi-observables are critical for finally determining the EoS of neutron-rich matter. Based on transport model simulations, several interesting predictions were made in the literature. Our review here on the isospin flows serves as an example of a broad scope of interesting physics one can study with nuclear reactions induced by neutron-rich nuclei. With the construction of various radioactive beam facilities around the world, we expect that comparisons of theoretical predictions with future data will allow us to better understand the isospin dependence of in-medium nuclear effective interactions. In particular, high-energy radioactive beams being available at some of the facilities will provide us with a great opportunity to explore the EoS of dense neutron-rich matter which is of vast interest to astrophysics. Well-concerted collective actions by both experimentalists and theoreticians will certainly move this field forward quickly.

We would like to thank the organizers and participants of the past three WCI conferences in Catania, Smith College and Texas A&M University for their great efforts in generating the collective flow of excitement and interest in the study of isospin physics with heavy ions. The work of M. Di Toro was supported in part by INFN Italy. The work of S.J. Yennello was supported in part by the Robert A. Welch Foundation grant No. A-1266 and the DOE grant No. DE-FG03-93ER40773. The work of B.A. Li was supported in part by the US National Science Foundation under grant No. PHYS0354572, PHYS0456890 and by the NASA-Arkansas Space Grants Consortium award ASU15154.

## References

1. H. Stöcker, W. Greiner, Phys. Rep. **137**, 277 (1986).
2. P. Danielewicz, Q. Pan, Phys. Rev. C **46**, 2002 (1992).
3. S. Das Gupta, G.W. Westfall, Phys. Today **46**, 34 (1993).
4. P. Danielewicz, Nucl. Phys. A **685**, 368c (2001).
5. P. Danielewicz, R. Lacey, W.G. Lynch, Science **298**, 1592 (2002) and references therein.
6. A.E.L. Dieperink, Y. Dewulf, D. Van Deck, M. Waroquier, V. Rodin, Phys. Rev. C **68**, 064307 (2003).
7. D. Vautherin, D.M. Brink, Phys. Rev. C **3**, 676 (1972).
8. H. Krivine, J. Treiner, O. Bohigas, Nucl. Phys. A **336**, 155 (1980).
9. E. Chabanat, P. Bonche, P. Haensel, J. Meyer, R. Schaefer, Nucl. Phys. A **627**, 710 (1997).
10. E. Chabanat, P. Bonche, P. Haensel, J. Meyer, R. Schaefer, Nucl. Phys. A **635**, 231 (1998).
11. F. Douchin, P. Haensel, J. Meyer, Nucl. Phys. A **665**, 419 (2000).
12. I. Bombaci, T.T.S. Kuo, U. Lombardo, Phys. Rep. **242**, 165 (1994).
13. I. Bombaci, Phys. Rev. C **55**, 1 (1997).
14. I. Bombaci, *EoS for isospin-asymmetric nuclear matter for astrophysical applications*, in *Isospin Physics in Heavy-ion Collisions at Intermediate Energies*, edited by Bao-An Li, W. Udo Schröder (Nova Science Publishers, New York, 2001) pp. 35-81 and references therein.
15. We remark here that also all relativistic mean-field approaches in the presently used approximation scheme are predicting a *stiff-like* symmetry term, proportional to the baryon density, coming from the  $\rho$ -meson field contribution, see ref. [16]. Actually a *superstiff-like* behaviour can be obtained when a coupling to the scalar charged meson  $\delta$  is added, see refs. [17–19].
16. S. Yoshida, H. Sagawa, N. Takigawa, Phys. Rev. C **58**, 2796 (1998).
17. S. Kubis, M. Kutschera, Phys. Lett. B **399**, 191 (1997).
18. B. Liu, V. Greco, V. Baran, M. Colonna, M. Di Toro, Phys. Rev. C **65**, 045201 (2002).
19. V. Greco, M. Colonna, M. Di Toro, F. Matera, Phys. Rev. C **67**, 015203 (2003).
20. B.-A. Li, C.M. Ko, W. Bauer, Int. J. Mod. Phys. E **7**, 147 (1998).
21. Bao-An Li, W. Udo Schröder (Editors), *Isospin Physics in Heavy-ion Collisions at Intermediate Energies* (Nova Science Publishers, New York, 2001).
22. M. Di Toro, V. Baran, M. Colonna, V. Greco, S. Maccarone, M. Cabibbo, Eur. Phys. J. A **13**, 155 (2002).
23. V. Baran, M. Colonna, V. Greco, M. Di Toro, Phys. Rep. **410**, 335 (2005).
24. M. Lopez-Quelle, S. Marcos, R. Niembro, A. Bouyssy, N. Van Giai, Nucl. Phys. A **483**, 479 (1988).
25. Bao-An Li, Nucl. Phys. A **681**, 434c (2001).
26. R.J. Furnstahl, Nucl. Phys. A **706**, 85 (2002).
27. L.W. Chen, C.M. Ko, B.-A. Li, Phys. Rev. Lett. **94**, 03701 (2005).
28. M. Prakash *et al.*, Phys. Rep. **280**, 1 (1997).
29. B.-A. Li, Phys. Rev. Lett. **85**, 4221 (2000).
30. P. Danielewicz, G. Odyniec, Phys. Lett. B **157**, 146 (1985).
31. B. Zhang, M. Gyulassy, C.M. Ko, Phys. Lett. B **455**, 45 (1999); P. Kolb, J. Sollfrank, U. Heinz, Phys. Rev. C **62**, 054909 (2000); V. Greco, C.M. Ko, P. Levai, Phys. Rev. C **68**, 034904 (2003); D. Molnar, S. Voloshin, Phys. Rev. Lett. **91**, 092301 (2003).
32. B.-A. Li, A.T. Sustich, Phys. Rev. Lett. **82**, 5004 (1999).
33. J.Y. Ollitrault, Phys. Rev. D **46**, 229 (1992).
34. P. Danielewicz, Nucl. Phys. A **673**, 375 (2000).
35. A.B. Larionov, W. Cassing, C. Greiner, U. Mosel, Phys. Rev. C **62**, 064611 (2000).
36. T. Gaitanos, C. Fuchs, H.H. Wolter, A. Faessler, Eur. Phys. J. A **12**, 421 (2001).
37. B.-A. Li, Z. Ren, C.M. Ko, S.J. Yennello, Phys. Rev. Lett. **76**, 4492 (1996).
38. G. Westfall, Nucl. Phys. A **630**, 27c (1998).
39. R. Pak *et al.*, Phys. Rev. Lett. **78**, 1022 (1997).
40. R. Pak *et al.*, Phys. Rev. Lett. **78**, 1026 (1997).
41. L. Scalone, M. Colonna, M. Di Toro, Phys. Lett. B **461**, 9 (1999).
42. The reduced impact parameter is defined as  $b_{red} \equiv b/b_{max}$ , where  $b_{max}$  is the sum of the two nuclear radii.
43. B.-A. Li, A.T. Sustich, B. Zhang, Phys. Rev. C **64**, 054604 (2001).
44. J. Rizzo, M. Colonna, M. Di Toro, V. Greco, Nucl. Phys. A **732**, 202 (2004).
45. B.-A. Li, B. Das Champak, S. Das Gupta, C. Gale, Nucl. Phys. A **735**, 563 (2004); B.A. Li, L.W. Chen, Phys. Rev. C **72**, 064611 (2005).
46. Bao-An Li, Phys. Rev. C **69**, 064602 (2004).
47. M. Di Toro, M. Colonna, J. Rizzo, *On the splitting of nuclear effective masses at high isospin density: reaction observables*, Argonne/MSU/JINA/RIA Workshop on Reaction Mechanisms for Rare Isotope Beams, edited by B. Alex Brown, AIP Conf. Proc., Vol. **791** (AIP, 2005) pp. 70-82; J. Rizzo, M. Colonna, M. Di Toro, Phys. Rev. C **72**, 064609 (2005).
48. W. Zuo, L.G. Cao, B.-A. Li, U. Lombardo, C.W. Shen, Phys. Rev. C **72**, 014005 (2005).
49. E.N.E. van Dalen, C. Fuchs, A. Fässler, Phys. Rev. Lett. **95**, 022302 (2005).
50. FOPI Collaboration (A. Andronic *et al.*), Phys. Rev. C **67**, 034907 (2003).
51. FOPI Collaboration (A. Andronic *et al.*), Phys. Lett. B **612**, 173 (2005).
52. V. Greco, Diploma Thesis (1997); V. Greco, A. Guarnera, M. Colonna, M. Di Toro, Phys. Rev. C **59**, 810 (1999); V. Greco, M. Colonna, M. Di Toro, A. Guarnera, Nuovo Cimento A **111**, 865 (1998).
53. P. Sapienza *et al.*, Phys. Rev. Lett. **87**, 2701 (2001).
54. C. Gale, G.F. Bertsch, S. Das Gupta, Phys. Rev. C **41**, 1545 (1990).
55. I. Bombaci *et al.*, Nucl. Phys. A **583**, 623 (1995).
56. V. Greco, V. Baran, M. Colonna, M. Di Toro, T. Gaitanos, H.H. Wolter, Phys. Lett. B **562**, 215 (2003); V. Greco, PhD Thesis (2002).
57. B.A. Li *et al.*, preprint nucl-th/0504069; AIP Conf. Proc. **791**, 22 (2005).
58. B.A. Li, G.C. Yong, W. Zuo, Phys. Rev. C **71**, 044604 (2005).